Isolation and Structural and Functional Characterization of Two Stable Peptic Fragments of Human α-Fetoprotein[†]

Igor Dudich,*[,‡] Natasha Tokhtamysheva,[‡] Lidia Semenkova,[‡] Elena Dudich,[‡] Jukka Hellman,[§] and Timo Korpela[||]

Institute of Engineering Immunology, Lyubuchany, Moscow Region, 142380, Russia, Turku Center for Biotechnology, Turku, Finland, and Joint Finnish−Russian Biotechnology Laboratory, Turku University, Finland FIN-20521

Received March 18, 1999; Revised Manuscript Received June 1, 1999

ABSTRACT: Short-time limited peptic hydrolysis of ligand-free human α-fetoprotein (AFP) gave two main fragments with molecular masses of 38 and 32 kDa, which had been produced by splitting of the molecule at the position Leu_{312}−Asn_{313}. A more prolonged proteolysis led to the further degradation of these fragments and appearance of highly proteolytically resistant 23-kDa (P23) and 26-kDa (P26) fragments, corresponding to N- and C-terminal parts of the AFP molecule, respectively. Comparative study of intact free of ligands AFP and isolated stable P23 and P26 fragments by circular dichroism, differential scanning calorimetry, and immunoprecipitation techniques demonstrated that these fragments conserved native secondary, tertiary; and antigenic structure, characteristic of the intact molecule. It was concluded that, free of ligands, the AFP molecule could be considered as a three-domain molecule, in which two compact rigid domains (N-terminal domain I and C-terminal domain III) are connected by relatively labile domain II. The structure of domain II could be approximated by a "molten globule" state, characterized by the absence of rigid tertiary structure but having a pronounced secondary structure. Tumor-suppressive activity via induction of apoptosis was recently shown for AFP [Dudich, E. I., et al. (1998) *Tumor Biol. 19*, 261−272]. We studied here the ability of isolated proteolytic AFP fragments to induce apoptosis in the AFP-sensitive Raji cell line, to determine possible localization of the active site responsible for apoptosis signaling. Unlike intact AFP, neither isolated fragments nor their equimolar mixture was able to induce apoptosis in a human lymphoma Raji cell line. However, it was demonstrated that both fragments P23 or P26 and their equimolar mixture P23 + P26 operated synergistically with intact AFP in suppression of Raji cell proliferation. These data suggested that two structurally determined requirements are necessary for AFP-mediated triggering of apoptosis: (i) dimerization of AFP to form the heterodimeric complex of C- and N-terminal domains and (ii) participation of the central part of AFP molecule (domain II).

α-Fetoprotein (AFP)[1] is a specific fetal and cancer-related 70-kDa glycoprotein consisting of 591 amino acid residues and 4% carbohydrates (*1*−*3*). AFP is normally secreted by embryonic tissues during prenatal development. AFP secretion is usually blocked in adults but becomes detectable at malignant cell transformation and cancer development (*1*). AFP can bind various biologically active ligands, such as arachidonic acid, steroids, estrogens, drugs, metals, etc., to deliver them into developing cells expressing AFP receptors (*4*−*6*). The biological role of AFP in embryogenesis and oncodevelopment remains to be elucidated, while a number of AFP activities, such as immunosuppression and up- and downregulation of cell growth, are now intensively studied (*7*−*17*). Tumor-suppressive activity of AFP was reported by various authors (*7, 9*−*16*) and has been recently shown to be closely related to apoptosis (*10*−*12*). AFP is capable of modulating various types of apoptosis, which are induced by TNF-α (*12*) or cellular adhesion and senescence (*15*).

AFP belongs to the serum albumin (SA) multigene family and exhibits 39% primary structure homology with SA (*18*), has a similar α-helical secondary structure (*19, 20*), and the general structure, stabilized by a sequence of 15 disulfide bonds (*18, 21*). The peculiarity of albumin-like proteins is the presence of three structurally homologous domains formed by two α-helical globin-like subdomains, which are cross-linked by interhelical disulfide bridges (*22, 23*). Such tertiary structure organization allows a diversity in protein structures depending on the presence of particular subdomain contacts that are conditioned by functional requirements. Numerous data obtained by limited proteolysis of SA have shown that interactions between individual subdomains are rather weak (*24*−*27*). This seems to be a characteristic feature of this protein, which allows binding of various ligands to fulfill its carrier function.

[†] This work is supported in part by International Science & Technology Center, ISTC (Grant 401).

* To whom correspondence should be addressed at the Institute of Engineering Immunology, Lyubuchany, Moscow Region, Chekchov District, 142380, Russia; Fax (7-095) 362-15-26; E-mail abramo01@ssw.alcoa.com.

[‡] Institute of Engineering Immunology.

[§] Turku Center for Biotechnology.

[||] Turku University.

[1] Abbreviations: AFP, α-fetoprotein; lfAFP, ligand-free α-fetoprotein; P38, P32, P26, and P23, fragments of α-fetoprotein with molecular masses of 38, 32, 26, and 23 kDa, respectively; SA, serum albumin; HSA, human serum albumin; BSA, bovine serum albumin; CD, circular dichroism; DSC, differential scanning calorimetry; TNF, tumor necrosis factor; ELISA, enzyme-linked immunosorbent assay; PAGE, polyacrylamide gel electrophoresis; SDS, sodium dodecyl sulfate; PVDF, poly(vinylidene difluoride).

10.1021/bi990630h CCC: $18.00 © 1999 American Chemical Society
Published on Web 07/27/1999

The method of limited proteolysis, which for years productively was used for structural and functional investigation of SA, has not yet been employed for structural studies of the AFP molecule. Peptic proteolysis of AFP was first engaged to determine the localization of copper binding sites (*28*), but structural and functional characterization of proteolysis products was not reported. Actually only one piece of experimental evidence supporting the domain and subdomain model of structural organization of the AFP molecule has been obtained by electron microscopy (*19*). It has been revealed that human AFP molecule has a "U-shaped" structure with three mass density regions, at both extremities and at a vertex of the molecule, and also that this mass map analysis correlates strongly with the subdomains organized by the disulfide bridges. However, it is not known whether topologically determined domains of the AFP molecule are structurally independent and could be separated without loss of their structural and/or functional properties. Moreover, recently it has been reported that differential scanning calorimetry did not reveal any domain structure for native AFP and no tertiary structure in the ligand-free AFP, which have been considered to be organized as a "molten globule" (*29*−*31*). Thus, experimental data available at present about the tertiary structure of AFP macromolecule are inconsistent and insufficient for understanding the mechanisms of its biological activity.

In this study we used the method of limited peptic proteolysis to unravel structural and functional properties of AFP molecule. Circular dichroism (CD) and differential scanning calorimetry (DSC) were used to determine the parameters characterizing the secondary and tertiary structure of AFP molecule and its proteolytic fragments were used to define the structural domains of AFP molecule, which could exist as thermodynamically independent cooperative subunits (*32*, *33*). Functional activity of intact AFP and its isolated peptic fragments was studied to determine the location of functional active sites of the AFP molecule, responsible for apoptosis signaling.

MATERIALS AND METHODS

α-*Fetoprotein Purification.* AFP was isolated from human cord serum by ion-exchange and immunoaffinity chromatography as described in refs *34* and *35* with minor modifications. Briefly, serum proteins were adsorbed on a DEAE-Sephacel column (5 cm × 30 cm) equilibrated with 20 mM sodium phosphate buffer with 0.1 M NaCl, pH 6.3, and then AFP was eluted with 0.2 M NaCl. Crude AFP-containing fractions in 0.05 M Tris-HCl and 0.5 M NaCl, pH 8, were passed through a set of three immunoaffinity columns: Sepharose-immobilized monospecific rabbit polyclonal anti-AFP antibodies, rabbit polyclonal antibodies against adult human serum proteins, and rat antibodies against rabbit immunoglobulins. Adsorbed AFP was eluted out in mild acid conditions by lowering of the pH the base buffer down to pH 5.0 by addition of 10 mM HCl. AFP solution was adjusted to pH 7.5 immediately after elution to conserve native protein structure. The purification was completed by gel chromatography on Ultrogel AcA 44. Purity of AFP was assessed by the ELISA Amerlite AFP-2T assay (Amersham), PAGE, and Rocket electrophoresis with monospecific antibodies against human AFP and adult serum proteins and was shown to be not less than 99.8%. Ligand-free AFP (lfAFP) was prepared by charcoal/HCl treatment, as described in ref *36*.

Antibodies and Antiserum. Polyclonal rabbit antiserum against AFP and adult human serum proteins and rat antiserum against rabbit IgG were obtained by standard immunization procedures. Monospecific polyclonal anti-AFP antibodies, those against adult human serum proteins, and anti-rabbit IgG were isolated from appropriate antiserum by passage through Sepharose CL-4B coupled with purified particular protein antigens.

Peptic Proteolysis of α-*Fetoprotein.* Proteolysis was performed at 20 °C in 0.1 M Gly-HCl buffer at pH 3.0 or in 0.1 M ammonium acetate buffer at pH 4.2. Freshly dissolved pepsin (Serva) at a concentration of 0.5% in 1 mM HCl was added to AFP solution (15−20 mg/mL) at an enzyme/AFP weight ratio of 1:1000 (at pH 3.0) or 1:100 (at pH 4.2). The reaction was stopped by the addition of 2 M Tris base to adjust the pH of the reaction mixture up to pH 7.5.

Purification of P23 and P26 Fragments. A peptic digest of AFP obtained in the course of a 3-h proteolysis at pH 4.2 and 20 °C was applied onto an Ultrogel AcA 44 column (2 cm × 90 cm) equilibrated with 10 mM sodium phosphate buffer, pH 6.5. The peak corresponding to a molecular mass of 20−30 kDa was collected and applied to a column of DEAE-Sephacel (2 cm × 15 cm) equilibrated with the same buffer. The column was eluted with a linear gradient of 0−0.5 M NaCl. Fractions corresponding to P23 and P26 fragments were collected, concentrated under nitrogen pressure on a PM10 membrane (Amicon) to a concentration of 10−15 mg/mL, and used for studies of structure and biological activity.

Determination of Protein Concentration. AFP concentration was determined spectrophotometrically at 278 nm by using an extinction coefficient $E_{1\%,278nm} = 5.3$ (*37*). Extinction coefficients for P23 and P26 fragments were determined spectrophotometrically, by evaluation of protein concentration by a Bradford assay with intact AFP as a standard (*38*), and were shown to be $E_{1\%,278nm} = 7.8 \pm 0.2$ and $E_{1\%,277nm} = 3.7 \pm 0.1$, respectively.

Polyacrylamide Gel Electrophoresis. SDS−PAGE of the total digest, column fractions, and purified fragments was performed according to the standard method of Laemmli using 12.5% (w/v) polyacrylamide gel with or without β_2-mercaptoethanol.

N-Terminal Amino Acid Sequence Determination. To assign the N-terminal amino acid sequences, the samples were electrophoresed on a polyacylamide gel and then electroblotted onto a poly(vinylidene difluoride) (PVDF) membrane (*39*). The bands corresponding to fragments with molecular masses of 38, 32, 27, 26, and 23 kDa were excised and subjected to N-terminal sequence analysis with a protein amino acid sequencer (Applied Biosystems model 477A/120A).

Double Immunodiffusion. Double immunodiffusion was carried out in 1% agarose gel in 20 mM sodium phosphate, pH 7.4, and 0.1 M NaCl. The central well contained 10 μL of anti-AFP rabbit antiserum and the outer wells contained 2 μL of a protein solution (1 mg/mL). After 48 h at 20 °C, the agarose slides were stained with Coomassie Blue (Serva) and analyzed.

Circular Dichroism Spectroscopy. Far-UV CD spectra of intact AFP and P23 and P26 fragments of AFP were recorded

on a J-500A spectropolarimeter (Jasco, Japan) equipped with a 1.0 mm temperature-controlled cell. All measurements were carried out in 20 mM sodium phosphate buffer, pH 7.4, containing 0.14 M NaCl, at 20 °C. Protein concentration was measured on a Shimadzu UV-2100 spectrophotometer (Japan). For all samples, concentration was in a range of 0.1−0.05 mg/mL. Protein spectra were corrected by subtraction of buffer spectrum. The mean residual molar ellipticity $[\Theta]_\lambda$ was calculated with a mean residual weight of amino acid equal to 112 for AFP and fragments (*18*). The α-helix content of all protein samples was estimated by the method of Provencher and Glöckner (*40*).

Differential Scanning Calorimetry. Calorimetric measurements were performed on a differential capillary scanning calorimeter DASM-4 equipped with cells of 0.464 mL working volume (Pushchino, Russia). Calorimetric runs were carried out at a heating rate of 1.0 °C/min. All measurements were carried out in 20 mM sodium phosphate buffer, pH 7.4, containing 0.14 M NaCl. The protein concentration was measured spectrophotometrically and for all samples was in a range of 2−4 mg/mL. The specific denaturation heat Q_d and specific transition excess heat capacity function $\langle \Delta C_{p,tr} \rangle$ (*32*, *33*) were calculated from the experimental calorimetry recording as described previously (*41*). Corresponding molar calorimetric enthalpy $\Delta H_{d,cal}$ was evaluated from electrophoretically determined molecular masses of AFP fragments. Experimental value of the denaturation temperature $T_{d,cal}$ was determined at the maximum of $\langle \Delta C_{p,tr} \rangle$ function.

Thermodynamic Analysis. The observed excess heat capacity function $\langle \Delta C_{p,tr} \rangle$ was deconvoluted into simple two-state transition constituents by the method suggested by Privalov and Potekhin (*33*) with some modifications, as described in ref *41*. According to this method, the number of cooperative melting transitions (n), temperature ($T_{d,i}$), and enthalpy ($\Delta H_{d,i}$) for each of $i = 1, 2, ..., n$ transitions were calculated by fitting the theoretical curve $\langle \Delta C_{p,tr} \rangle$ to the experimental one. The equations describing theoretical excess heat capacity function $\langle \Delta C_{p,tr} \rangle$ were taken from ref *33*.

Cell Growth Inhibition Assay. An AFP-sensitive human Burkitt lymphoma Raji cell line was used to test cell growth regulative activity of AFP and its proteolytic fragments. Cells were maintained in RPMI-1640 media supplemented with L-glutamine and 10% fetal calf serum (FCS) in a humidified 5% CO_2 atmosphere. Prior to addition of reagents, cells were washed with the medium, plated on 96-well polystyrene plates (Costar) at a density of 3×10^3 cells/well in 180 μL of complete medium, and incubated for 2 h. Then 20 μL of solution of AFP or fragments in the phosphate-buffered saline (PBS) with appropriate protein concentration were added in each well and incubated for 20 h. For the last 4 h of incubation, 1 μCi of [^{3}H]thymidine (1 Ci/mmol) was added into the each well. The experimental data were expressed as a percentage of [^{3}H]thymidine incorporation in experimental cell cultures relative to the control ± SD from triplicate cultures, as described (*12*). Intact cell cultures incubated in medium without additions were taken as a control.

RESULTS

Digestion of AFP with Pepsin. Electrophoretic patterns of typical peptic digests of AFP at pH 4.2, 20 °C, for various reaction times are shown in Figure 1. Short-time (0.5-h) proteolysis of AFP yielded main electrophoretic bands corresponding to molecular masses of 38 ± 1 kDa (P38), 32 ± 1 kDa (P32), and 27 ± 1 kDa (P27) (lane c). At this stage of proteolysis some amount of undigested AFP was still seen at a position corresponding to 69 kDa. The long-term proteolysis (3 h) led to the complete degradation of P38 and P32 fragments with appearance of fragments with molecular masses of 26 ± 1 kDa (P26), 23 ± 1 kDa (P23), and 12 ± 1 kDa (lane d). Final fragments P26 and P23 were highly resistant to further degradation, while fragment P12 quickly disappeared. Figure 2 shows the relative content of intact AFP and its fragments in the reaction mixture at various pH values as a function of the reaction time. Values of half-digestion time for intact AFP and fragments assessed from kinetic data are shown in Table 1. It is seen that proteolytic stability of P26 and P23 fragments was significantly higher than that determined for P38, P32, and intact AFP independently on pH of the reaction mixture (Figure 2).

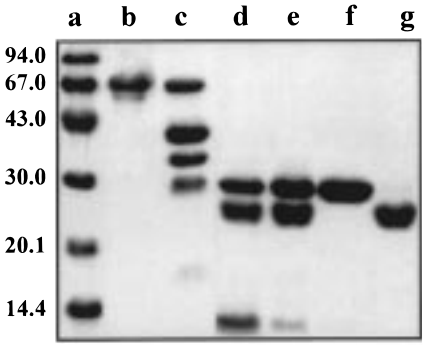

FIGURE 1: SDS−polyacrylamide gel electrophoresis of peptic digests of human AFP (AFP:pepsin = 100:1, pH 4.2, 20 °C) in the presence of β_2-mercaptoethanol. Lane a, molecular mass standards (phosphorylase B, bovine albumin, ovalbumin, carbonic anhydrase, trypsin inhibitor, and α-lactalbumin); lane b, intact AFP; lane c, 0.5-h digest; lane d, 3-h digest, lane e, 20−30 kDa fraction after gel filtration through a Ultrogel AcA 44 column; lane f, fraction 1 from a DEAE-Sephacel column, corresponding to fragment P23; lane g, fraction 2, corresponding to fragment P26 (Figure 3B), eluted by a linear 0−0.5 M NaCl gradient from a DEAE-Sephacel column.

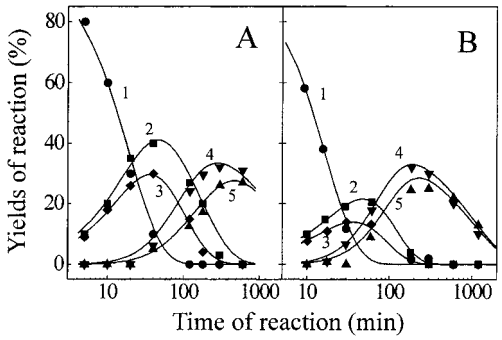

FIGURE 2: Kinetics of the process of pepsin degradation of AFP (1) and its fragments P32 (2), P38 (3), P23 (4), and P26 (5). Limited peptic proteolysis was performed in 0.1 M Gly-HCl, pH 3.0, with an AFP:pepsin ratio of 1000:1 (panel A) or in 0.1 M ammonium acetate buffer, pH 4.2, 20 °C, with initial ratio of AFP:pepsin = 100:1 (panel B). The data are expressed as a percentage of the individual fragment content relative to the total protein amount in the digest as assessed from SDS−PAGE data analysis.

Location of Peptides in AFP Sequence. N-Terminal amino acid sequences determined for peptic AFP fragments are summarized in Table 2, where the values of molecular weight

Table 1: Half-Digestion Time for AFP and Its Peptic Fragments[a]

	half-digestion time (h)				
pH	AFP	P38	P32	P26	P23
3.0	0.3	2.7	1.3	30	34
4.2	0.4	0.8	0.5	17	20

[a] Proteolysis was performed at 20 °C in 0.1 M Gly-HCl buffer at pH 3.0 with a pepsin:AFP weight ratio of 1:1000 or in 0.1 M ammonium acetate buffer at pH 4.2 with a pepsin:AFP weight ratio of 1:100.

assessed from SDS−PAGE data are also shown. It is seen that fragments P38, P27, and P23 are heterogeneous, but their N-terminus positions are very close to each other's. The positions of peptic fragments in the sequence of human AFP (*2, 18*) were evaluated according to determined N-terminal sequences. It was also shown that N-terminal sequence Arg-Thr-Leu-His-Arg-Asn-Glu-Tyr-Gly-Ile, determined here for the intact embryonic human AFP molecule, is the same as that obtained for cancer-related AFP, derived from the culture medium of AFP-secreting human hepatoma cell line HepG2 (*2*). It was demonstrated in ref *2* that HepG2-derived AFP has an unconsidered earlier first amino acid residue Arg and thus the complete amino acid sequence of AFP includes 591 rather than 590 residues. Our data corroborated the results of Pucci et al. (*2*) that embryonic AFP, similarly to tumor-derived AFP, has 591 amino acid residues. Therefore, we used the numeration of amino acids for AFP as in ref *2*.

The molecular weights and N-terminal amino acids of the AFP fragments indicate that initially pepsin caused cleavage of AFP at the position Leu_{312}−Asn_{313} to produce two fragments corresponding to N-terminal (P38) and C-terminal (P32) parts of the molecule. At the more prolonged digestion, fragment P38 lost about 15 kDa from the C-terminal part and changed into fragment P23. Similarly, P32 gradually shortened from the N-terminal end and turned first to P27 and then to P26.

Purification of Stable Fragments P23 and P26. AFP fragments have been isolated by a combination of gel chromatography on Ultragel AcA 44 (Figure 3A) and ion-exchange chomatography on DEAE-Sephacel (Figure 3B). The main peak, containing approximately 50% of the total protein, corresponding to a molecular mass of 20−30 kDa (Figure 3A), was collected and applied to a DEAE-Sephacel column. According to SDS−PAGE (Figure 1, lane e), this fraction mainly consisted of fragments P23 and P26. These fragments have been recovered from DEAE column after elution with a linear gradient of 0−0.5 M NaCl. Figure 3B shows that the elution profile represented two well-resolved peaks with maxima at 0.17 M (peak 1) and 0.3 M NaCl (peak 2). These peaks, containing pure fragments P23 (peak 1) and P26 (peak 1) (Figure 1, lanes f and g), were collected and concentrated.

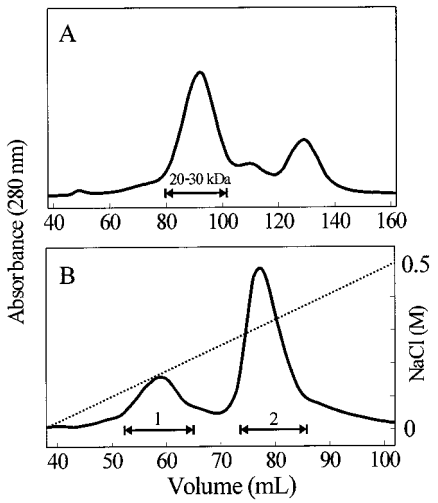

FIGURE 3: Purification of P26 and P23 peptic fragments of AFP. Panel A: Gel chromatography pattern of a 3-h peptic digest of human AFP (pH 4.2) through a column (2.5 × 90 cm) of Ultrogel AcA 44, equilibrated with 10 mM sodium phosphate buffer, pH 6.5. The first peak, corresponding to a molecular mass of 20−30 kDa, was collected and applied onto a DEAE-Sephacel column in the same buffer. Panel B: Ion-exchange chromatography of the 20−30 kDa fraction on DEAE-Sephacel. The column was eluted with a linear gradient of 0−0.5 M NaCl. Fractions corresponding to pure fragments P26 (peak 1) and P23 (peak 2) are shown by arrows.

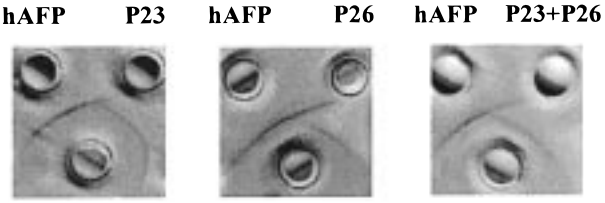

FIGURE 4: Double immunodiffusion patterns of intact human AFP and its peptic fragments P23, P26, and their equimolar mixture P23 + P26. The central well contained monospecific rabbit antiserum against human AFP. The positions of the wells with corresponding samples are indicated in the pattern.

Antigenic Properties of Isolated Fragments. Antigenic properties of isolated fragments of AFP were tested by the Ouchterlony double immunodiffusion technique with rabbit antiserum to AFP (Figure 4). Fragments P23 and P26 formed continuous precipitation lanes with the anti-AFP antiserum, showing the presence of antigenic determinants in common with those of intact AFP in tested protein samples. However, single spurs between AFP (upper left wells) and each isolated fragment P23 or P26 (upper right wells) indicated the absence

Table 2: Characterization of AFP Peptic Fragments

fragment	mol. mass[a] (kDa)	N-terminal sequence	N-terminal position[b]	relative amount (%)
P38	38	Arg-Thr-Leu-His-Arg-Asn-Glu-Tyr-Gly-Ile	1	50
P38	38	His-Arg-Asn-Glu-Tyr-Gly-Ile-Ala-Ser-Ile	4	50
P32	32	Asn-Arg-Phe-Leu-Gly-Asp-Arg-Asp-Phe-Asn	313	100
P27	27	Val-Ile-Leu-Arg-Val-Ala-X-Gly-Tyr-Gln	351	80
P27	27	X-Gly-Tyr-Gln-Glu-Leu-Leu-Glu-X−X	357	20
P26	26	Leu-Glu-Lys-X-Phe-Gln-Thr-Glu-Asn-Pro	363	100
P23	23	Asp-Ser-Tyr-Gln-X-Thr-Ala-Glu-Ile-Ser	12	60
P23	23	Ser-Ile-Leu-Asp-Ser-Tyr-Gln-X-Thr-Ala	15	40

[a] The values of molecular mass were assessed from SDS−PAGE data. [b] The numeration of amino acids for AFP is as in ref *2*.

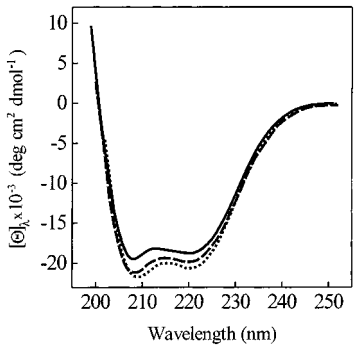

FIGURE 5: Far-UV CD spectra of intact AFP (solid line) and its peptic fragments P23 (dashed line) and P26 (dotted line) at 20 °C. All measurements were carried out in 20 mM sodium phosphate buffer, pH 7.4, containing 0.14 M NaCl. Protein concentrations were 0.095 ± 0.008 mg/mL for AFP, 0.060 ± 0.005 mg/mL for P26, and 0.082 ± 0.005 mg/mL for P23.

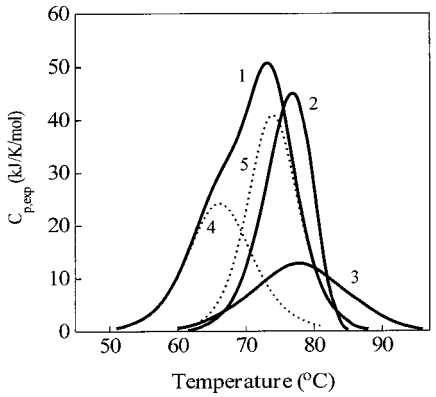

FIGURE 6: Temperature dependencies of the molar transition excess heat capacity $\langle \Delta C_{p,tr} \rangle$ of the ligand-free AFP (1), fragment P26 (2), and fragment P23 (3). Experimental data are shown by solid lines. Theoretically calculated curves, representing the individual cooperative thermodynamic transitions, obtained by deconvolution analysis (*33*, *41*) of the melting curve for intact AFP, are shown by dotted lines 4 and 5. All measurements were carried out in 20 mM sodium phosphate buffer, pH 7.4, containing 0.14 M NaCl. Protein concentrations were 3.81 ± 0.05 mg/mL for AFP, 2.87 ± 0.07 mg/mL for P26, and 3.11 ± 0.07 mg/mL for P23.

of some antigenic determinants of intact AFP in each fragment. Double immunodiffusion analysis of the equimolar mixture of isolated peptic fragments of AFP (right pattern, top right well) also demonstrated only a partial identity with AFP, indicating that some antigenic sites were removed by proteolysis. However, these results showed that limited peptic proteolysis conserved main antigenic sites characteristic of the intact AFP molecule.

Analysis of Secondary Structure of AFP and Its Fragments by Circular Dichroism Spectroscopy. Figure 5 shows CD spectra of intact AFP (solid line) and its peptic fragments P26 (dotted line) and P23 (dashed line) at neutral pH at 20 °C. The shape and intensity of the CD spectrum of intact AFP is typical of all-α-helical proteins (*42*). The α-helix content calculated by the method of Provencher and Glöckner (*40*) for our AFP sample was 65%. It is practically identical to that found by Zizkovsky et al. (*20*) (67%), but is higher than that reported for human AFP (49%) by Luft and Lorscheider (*19*). The CD spectra of P26 and P23 fragments were very similar in form and intensity to that of intact AFP (Figure 5). The α-helix content estimated for P23 and P26 fragments was 68% and 71%, respectively. This indicated the high degree of native conformation of both fragments, showing that the proteolysis and isolation procedure did not disturb their secondary structure. This in turn gave us the possibility to appreciate the secondary structure of the digested part of the AFP. The mean residual molar ellipticity $[\Theta]_{222}$ for the digested part of the AFP was evaluated as a difference between $[\Theta]_{222}$ of intact AFP and that for fragments P26 and P23 and was equal to 16 500. This allows us to estimate α-helical content of this part of AFP as the value of 50−55% and shows that the central part of the AFP macromolecule, which is digested in the course of the long-time peptic proteolysis, has a pronounced secondary structure.

Tertiary Structure Analysis of AFP and Its Peptic Fragments by Differential Scanning Calorimetry. Figure 6 shows the experimental temperature dependencies of the transition excess heat capacity function $\langle \Delta C_{p,tr} \rangle$ of ligand-free AFP and its fragments P26 and P23. These melting curves revealed endothermic denaturation in the temperature range of 70−80 °C for all samples. The melting curve of AFP had a distinct shoulder near 65 °C (Figure 6, curve 1). The deconvolution analysis of the melting curve for intact AFP revealed two independent transitions (curves 4 and 5), showing the existence of two thermodynamically independent cooperative units, which could correspond to separate structural domains. The values of the specific heat of denaturation Q_d and corresponding values of molar calorimetric enthalpies $\Delta H_{d,cal}$ are represented in Table 3. It is seen that the denaturation enthalpy $\Delta H_{d,cal}$ of AFP (661 kJ/mol) in the limit of experimental accuracy (5−7%) is equal to the sum of enthalpies of the P23 and P26 fragments (677 kJ/mol). This suggests that P23 and P26 fragments are tightly packed and retain their native tertiary structure, similar to that in the content of the intact AFP molecule. The calculated values of transition enthalpies for each of the two thermodynamically independent transitions (290 and 414 kJ/mol) are close to the experimental values of the enthalpies obtained for isolated P23 and P26 fragments (231 and 430 kJ/mol, respectively). Thus, it can be proposed that the low-temperature transition corresponds to the melting of N-terminal domain I and the high-temperature transition to the melting of C-terminal domain III. The theoretical curve calculated for the second transition (Figure 6, curve 5) practically completely coincided with the experimental melting curve obtained for the isolated P26 fragment (corresponding to domain III), showing the conservancy of the tertiary structure conformation in P26. Taking into account the 10 °C difference between the values of the denaturation temperature for the first transition of intact AFP (calculated value, Figure 6, curve 4) and fragment P23 (Figure 6, curve 3), it could be noted that the isolated P23 fragment, corresponding to N-terminal domain I, has higher thermostability than that in the content of the intact AFP molecule.

Isolated Fragments P23 or P26 Can Inhibit Raji Cell Proliferation Only in the Presence of Intact AFP. Earlier we have shown that human AFP is capable of inducing dose-dependent growth inhibition and programmed cell death in different human tumor cell lines (*10*−*12*, *15*, *16*). Figure 7 demonstrates the effect of intact AFP and its isolated peptic fragments P23 and P26 on the proliferation of human Raji cell line. Incubation of Raji cells with AFP induced a strong

Table 3: Thermodynamic Parameters of Ligand-Free AFP, P26, and P23 Fragments

	experimental[a]				theoretical[b]			
sample	Q_d (J/g)	$T_{d,cal}$ (^{o}C)	$\Delta H_{d,cal}$ (kJ/mol)	M (kDa)	n	$T_{d,i}$ (^{o}C)	$\Delta H_{d,i}$ (kJ/mol)	m (kDa)
lfAFP	9.58	73.2	661	69	2		704	70
first transition						66.0	290	
second transition						73.8	414	
P23	9.87	77.7	237	23	1	77.9	231	22
P26	16.30	77.5	440	26	1	76.3	430	25

[a] Experimental parameters Q_d and $T_{d,cal}$ were obtained by direct DSC measurements. Values of $\Delta H_{d,cal}$ were calculated from Q_d by using electrophoretically determined molecular masses M. The experimental errors in the values of $T_{d,cal}$ were about ± 0.3 ^{o}C, while in Q_d and $\Delta H_{d,cal}$ they were less than $\pm 8\%$. [b] Theoretical parameters m, n, $\Delta H_{d,i}$, and $T_{d,i}$ were calculated from a mathematical model of the temperature denaturation process (*33*). The values of the parameters, shown in the table, were obtained from the best fitting of the theoretically calculated function $\langle \Delta C_{p,tr}(T, m, n, \Delta H_{d,i}, T_{d,i}) \rangle$ to the experimental data. The errors in the theoretical parameters did not exceed 10%.

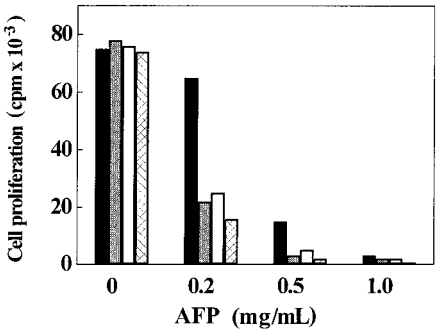

FIGURE 7: Raji cell growth suppression induced by isolated fragments P23 (open bars), P26 (gray bars) and the mixture of P23+P26 (cross-hatched bars) in the presence of various doses of intact AFP. Concentration of the fragments was 1 mg/mL. Cells incubated with intact AFP without addition of fragments were taken as a control (black bars). Raji cells (3×10^3 cells/well) were incubated with addition of various doses of AFP and fragments and assessed for their [^{3}H]thymidine incorporation for the last 4 h of culture. The data were calculated as a mean for three independent experiments: SD was less than 5%.

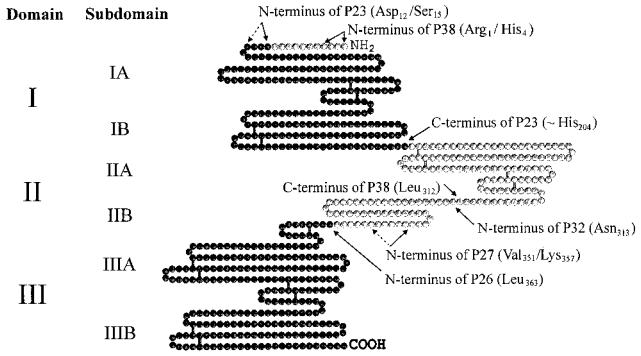

FIGURE 8: Schematic structure of the human AFP molecule and its peptic fragments. The sequence assignment and the disulfide bridge patterns are taken from refs *2* and *17*. Short-time limited peptic proteolysis splits human AFP at a position Leu$_{312}$−Asn$_{313}$, giving 38-kDa (P38) and 32-kDa (P32) fragments. Proteolytically stable 23-kDa (P23) and 26-kDa (P26) fragments, corresponding to N- and C-terminal parts of the AFP molecule, are shown in black. Dotted arrows indicate the alternative splitting sites of heterogeneous fragments P38, P27, and P23.

dose-dependent growth inhibition. In contrast, isolated peptic fragments P23 and P26 and their equimolar mixture P23 + P26 did not show any significant inhibitory activity. To determine the causes of the loss of the biological activity of P23 and P26 fragments, we studied the growth-inhibitory activity of the mixtures of various doses of AFP with isolated fragments P23 and P26 or the mixture P23 + P26. Figure 7 shows that addition of P23 or P26 fragments to the intact AFP significantly enhanced total cytotoxic effect. Moreover, both fragments P23 or P26 and their equimolar mixture P23 + P26 operated synergistically with a suboptimal dose of intact AFP (0.2 mg/mL) in suppression of Raji cell proliferation. Indeed, the value of $ID_{50\%} \approx 0.15$ mg/mL assessed from the growth dependence curves for the mixtures AFP + P23 or AFP + P26 is significantly less than that obtained for the intact AFP alone (0.35 mg/mL) (data not shown). These data show that AFP enhanced cell sensitivity to growth-suppressive activity of isolated fragments. This suggests the interaction between AFP and its fragments, resulting in formation of heterodimeric complexes, which seems to be necessary for the formation of an active site, responsible for triggering of apoptotic signaling.

DISCUSSION

Characteristics of Limited Peptic Proteolysis of Human AFP. Despite the structural homology of AFP and HSA, pepsin fragmentation studies involving human AFP demonstrated some striking differences in structural organization of these proteins. Limited peptic proteolysis of HSA yielded a rather complicated set of overlapping and rapidly degrading fragments (*24*−*27*). To obtain relatively large HSA fragments, proteolysis was usually carried out in the presence of bound ligands, which can affect significantly the tertiary structure of the molecule and can induce essential changes in the pattern of enzymatic fragmentation (*26*). The long-time experience on the studies of proteolytic fragmentation of SA allows one to conclude that practically all inter- and extradomain parts easily undergo proteolytic cleavage as well as intrasubdomain portions, especially in subdomain IIIA (*27*).

In contrast to SA, the process of peptic fragmentation of human AFP occurred more simply: the central part of the molecule, i.e., domain II according to the model proposed in ref *18*, rapidly degraded with the subsequent formation of fragments, corresponding to domains I and III, which were highly resistant to the further proteolysis. The simple mode of fragmentation and significant stability of two terminal fragments allowed to receive an extremely high yield of these fragments, reaching 70% of theoretical quantity. Figure 8 shows the main proteolytic cleavage sites on the AFP molecule determined here. The peptic cleavage of the central domain II included two separate stages. At the first stage, pepsin caused cleavage of human AFP molecule at a position between Leu$_{312}$ and Asn$_{313}$ to produce two halves of the molecule (fragments P38 and P32). The bond 312−313 is located in the peptide region providing intradomain connec-

Table 4: Structural Characteristics of Intact AFP and Its Domains

parameters	lfAFP	N-terminal domain I	C-terminal domain III	middle domain II
mol. mass[a] (kDa)	69	23	26	20
mol. mass cal[b] (kDa)	70	22	25	23
$E_{1\%,278\ nm}$	5.3	7.8	3.7	
relative peptic stability[c] (h)	0.4	20	17	0.5−0.8
$[\Theta]_{222}$[d] (deg·cm^2·mol^{-1})	19000	19900	20100	16500
α-helix content[e] (%)	65	68	71	55
Q_d (J/g)	9.58	9.87	16.3	0
no. of cooperative thermodynamic domains	2	1	1	0
$\Delta H_{d,cal}$ (kJ/mol)	661	227	424	0
$T_{d,cal}$ (°C)	73.2	77.7	77.5	

[a] Determined by polyacrylamide gel electrophoresis. [b] Determined from the best fitting of the theoretically calculated function $\langle \Delta C_{p,tr}(T, m, n, \Delta H_{d,i}, T_{d,i}) \rangle$ to the experimental DSC data. [c] Half-digestion time in 0.1 M ammonium acetate buffer at pH 4.2 with an enzyme/protein weight ratio of 1:100 at 20 °C. [d] The mean residual molar ellipticity $[\Theta]_{222}$ for domain II was evaluated as a difference between these values for intact AFP and its fragments P26 and P23. [e] Secondary structure was evaluated from CD spectra as in ref *40*. β-Structure content in all samples was determined to be zero; the errors were about 8%.

tion of subdomains IIA and IIB (the designations are taken from ref *23*). The same position in various species of SA is also very sensitive to enzymatic proteolysis. Thus, in HSA this position corresponds to AA residues 308−309 and in BSA to 306−307, respectively (*24*−*27*). Immediately after splitting of the intraresidual bond 312−313 there occurred rapid partial breakdown of fragment P38 by cutting off the subdomain IIA and of fragment P32 by degradation of part of subdomain IIB, corresponding to the sequence 313−362, which does not contain disulfide bonds. Partial degradation of P38 and P32 fragments yielded two fragments stable to further proteolysis: fragments P23 (corresponds to N-terminal domain I) and P26 (corresponds to C-terminal domain III). Fragments with molecular masses of 36 and 22 kDa have been obtained by Bayard et al. (*28*) and were characterized for their copper binding properties. These fragments evidently corresponded to P38 and P23 obtained here, representing the N-terminal part of the AFP molecule. The results of the limited peptic proteolysis of AFP are in good agreement with DSC data, demonstrating that the tertiary structure of the AFP molecule is composed of two tightly packed cooperative N- and C-terminal domains, which are connected by labile and proteolytically unstable domain II.

Comparative Structural Analysis of Intact AFP and Its Fragments. Results obtained in structural and proteolytic studies of human AFP and its fragments allowed us to make certain conclusions about the structural characteristics of structural domains in the content of the intact AFP molecule. Main structural data obtained here for the ligand-free AFP and its domains are summarized in Table 4. It is seen that the three domains of AFP molecule have rather similar secondary structure parameters but differ significantly in their tertiary structure characteristics, reflected in the differences in the values of denaturation enthalpies and relative peptic stabilities obtained for various AFP fragments.

Characteristic Structural Features of Fragment P23. Subdomain IA, which is an N-terminal part of fragment P23, has only two disulfide bonds (*1, 18*), lacking the other two S−S bonds. They are supposed to be necessary to stabilize the N-terminal peptide, composed of 80 amino acid residues, which is not locked by the two-loop construction, as in other "A" subdomains of the molecule. This indicates a possible presence of intermolecular lability in this part of domain I (*18*). Electron microscopic data demonstrated certain structural heterogeneity in this region, which could be accounted for by the increased interchain lability (*19*). On the other hand, our data demonstrated that AFP loses only 12 or 15 of the initial N-terminal residues in the course of 3-h proteolysis (Table 2), which constituted only a small part (about 20%) of the unlocked with disulfide bonds N-terminal peptide. In the course of peptic hydrolysis, HSA loses 48 N-terminal residues (47 for BSA) (*24*−*27*). This could be connected with the absence of one disulfide bond, allowing the polypeptide chain 1−52 to be free. Hence, in the absence of two disulfide bonds, subdomain IA of AFP is very stable and has a significant structural rigidity in comparison with the corresponding part of HSA molecule. It should be emphasized that especially this part of AFP molecule has significant differences in amino acid sequence as compared to HSA (only 16% homology in comparison with the total AFP/HSA homology of 39%) (*18*). DSC and CD results demonstrated the remaining native secondary and tertiary structure of P23. Moreover, taking into account that temperature of denaturation obtained for P23 fragment (Figure 6, curve 3) was 12 °C higher than that obtained for the domain I within the intact AFP molecule (Figure 6, curve 4), it could be suggested that domain II certainly destabilizes the tertiary structure of domain I.

Characteristic Structural Features of Fragment P26. The N-terminal residue of the P26 fragment is Leu_{363} and thus this fragment includes, besides the whole domain III, additionally a part of the subdomain IIB, formed by a C-terminal disulfide bond (see Figure 8). Taking into account that the long-time proteolysis failed to split this IIB subdomain loop, this additional loop can be considered as an intrinsic part of domain III. Thus, domain III of the AFP molecule, represented by fragment P26, is stabilized by seven interchain disulfide bonds. It was shown that domain III of AFP has the highest identity with the corresponding domain of HSA (48% homology) (*18*). However, our results indicate an essential difference between tertiary structures of these domains in HSA and AFP. Indeed, in various samples of SA, the most reachable proteolytic sites are located in the positions of inter- and intradomain connections, whereas subdomains are more stable to proteolysis with the exception of subdomain IIIA of HSA, which could be easily cleaved by pepsin in position 422−423 (*26*), because the most active ligand-binding cavity is located there (*23*). In contrast to HSA, domain III of AFP is the most resistant part to proteolytic degradation and heat denaturation. It is noteworthy that the specific enthalpy of denaturation Q_d of fragment P26 overcame significantly the Q_d value obtained for the intact AFP molecule (Table 3), demonstrating the increased thermostability for domain III of AFP.

Characteristic Structural Features of AFP Domain II. The part of the AFP molecule that is deleted in the course of the long-time peptic proteolysis practically completely coincides with domain II (Figure 8) with the exception of the C-terminal loop of the domain, which is included in fragment P26. Figure 8 shows that subdomain IIA is stabilized by two

double loops (between Cys_{206} and Cys_{295}), whereas in subdomain IIB (*296*−*362*) there are no internal disulfide bonds. It was first proposed by Morinaga et al. (*18*) and discussed later by other authors (*19*−*22, 43, 44*), that the C-terminal part of domain II could be considered as a flexible "hinge region". Our data support this hypothesis, demonstrating that actually both subdomains IIA and IIB are easily degraded by pepsin, as well as the most accessible part of the molecule in position 312−313, which is located in the peptide connecting these subdomains. Calorimetric results demonstrated that domains I and III give the main contribution to the total heat denaturation of intact AFP, whereas domain II has a denaturation enthalpy practically equal to zero (Table 4). Simultaneously, it was demonstrated by CD that domain II has a pronounced α-helical secondary structure. This means that domain II of AFP molecule has the conformation of the so-called "molten globule" state. Such a conformation was described for many globular proteins under mild denaturing conditions and is characterized by the relatively high lability of the tertiary structure with simultaneous maintenance of the compactness of the general structure, typical of the native protein conformation (*45, 46*). In the case of AFP, the molten globule state of domain II could be necessary for the regulation of the overall protein structure by the ligand molecules (*29, 47, 48*). It was demonstrated that the ligand binding site is located in subdomain IIA in the vicinity of Lys_{224} (*4*) as well as of the site of glycosylation at Asn_{233} (*18*). It might be suggested that in the absence of ligands, the sugar residues could provide conditions for maintaining the molten globule state by simulation of mild denaturing conditions by screening the certain amino acid residues in the ligand binding site.

Structural Requirements for the Functional Activity of AFP. Comparative study of the functional activity of intact AFP and its fragments for their ability to induce apoptosis in human lymphoma Raji cells demonstrated that (i) intact AFP induced strong dose-dependent growth arrest of Raji cells; (ii) isolated P23 and P26 fragments or their equimolar mixture were unable to induce growth inhibitory effects in these cells; (iii) in the presence of low concentrations of AFP, fragments P23 and/or P26 became functionally active and induced growth inhibition in Raji cells, in a similar manner as intact AFP at required doses. This suggested that triggering of apoptosis by isolated fragments in the presence of intact AFP could be induced by the heterooligomeric macromolecular complexes, formed by AFP and its fragments. On the basis of the structural and functional data of this study a model can be proposed of the formation of the identical functionally active AFP−P23 and AFP−P26 complexes, when fragment P23 (domain I) interacts with the C-terminal part of the intact AFP molecule (domain III) and, otherwise, fragment P26 (domain III) interacts with the N-terminal domain of AFP (domain I). This is the only way when, independent of the kind of added fragments (P23 or P26), the same structure could be formed, including the complex of domain I and domain III (Figure 9B,C). However, taking into consideration the fact that the equimolar mixture of isolated fragments P23 and P26 was unable to induce apoptosis, it can be concluded that, for apoptosis triggering, the presence of domain II of AFP is necessary. Our recent data demonstrate that AFP can induce apoptosis at concentrations exceeding 0.1−0.2 mg/mL (*10, 11*). At lower doses

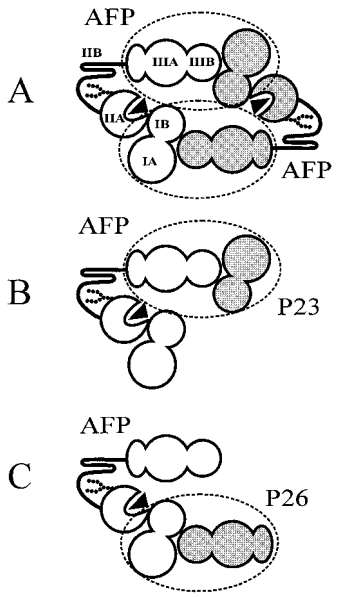

FIGURE 9: Hypothetical model of AFP/AFP homodimers (A) and heterodimeric complexes of AFP/P23 (B) and AFP/P26 (C). According to the model, the active site, responsible for the apoptosis induction, is formed by a heterodimeric complex of C- and N-terminal domains of AFP (shown by dotted line). Domain II, the structure of which is affected by bound ligands and sugar moiety (which are shown on the domain IIA by symbols), also participates in formation of the apoptotic active site. By gray color are shown the secondary molecular participants (fragments or entire AFP molecule), introduced in the formation of the complex active site.

AFP does not suppress tumor cell growth (*10*). Additionally we have demonstrated by analytical ultracentrifugation and DSC that at concentrations of more than 0.5−1.0 mg/mL the dimerization of AFP occurs (*48*). Therefore, for AFP-mediated induction of apoptosis in tumor cells, the formation of a particular kind of homodimeric complex, in which domain I interacts with domain III, is necessary (Figure 9A). Similar dimeric construction was found to be a basic unit of the molecular crystals of HSA (*23*), demonstrating that for the albumin-like structure this mode of dimerization is energetically favorable. It has been demonstrated recently that AFP causes apoptosis in tumor cells via activation of caspase-3 and independently on Fas/FasL and TNF/TNF-receptor-dependent signaling (*49*). But it is not clear yet if this death signal is triggered by activation of specific membrane AFP receptors or initiated by AFP binding to the unknown cytosolic receptor molecules involved in apoptosis signaling. However, our data demonstrated the necessity of oligomerization of corresponding apoptosis-associated receptors by specific binding with dimeric AFP complexes to induce apoptosis in tumor cells, supporting the hypothesis of AFP dimerization with unknown cytosolic proteins, leading to the modulation of various growth regulative and apoptotic signals discussed by Misejewsky (*43, 44*). Taken together, these results suggest that two structurally determined requirements are necessary for apoptosis signaling by AFP molecular complexes: (i) formation of heterodimeric complex of C- and N-terminal domains of AFP and (ii) participation of the central part of the AFP molecule (domain II).

REFERENCES

1. Deutsch, H. F. (1991) *Adv. Cancer Res. 56*, 253−312.

2. Pucci, P., Siciliano, R., Malorni, A., Marino, G., Tecce, M., F., Ceccarini, C., and Terrana, B. (1991) *Biochemistry 30*, 5061−5066.
3. Yamashita, K., Taketa, K., Nishi, S., Fukushima K., and Takashi O. (1993) *Cancer Res. 53*, 2970−2975.
4. Nishihira, J., Koyama, Y., Sakai, M., and Nishi, S. (1993) *Biochem. Biophys. Res. Commun. 196*, 1049−1057.
5. Uriel, J., Torres, J.-M., and Anel, A. (1994) *Biochim. Biophys. Acta 1220*, 231−240.
6. Shin, W. S., Yamashita, H., and Hirose, M. (1994) *Biochem. J. 304*, 81−86.
7. Jacobson, H. I., Bennett, J. A., and Mizejewski, G. J. (1990) *Cancer Res. 50*, 415−420.
8. Semeniuk, D. J., Boismenn, R., Tam, J., Weissenhofer, W., and Murgita, R. A. (1995) *Exp. Med. Biol. 383*, 255−269.
9. Bennett, J. A., Semeniuk, D. J., Jacobson, H. I., and Murgita, R. A. (1997) *Breast Cancer Res. Treatment 45*, 169−179.
10. Dudich, E. I., Semenkova, L. N., Gorbatova, E. A, Dudich, I. V., Khromikh, L. M., Grechko, G. K., and Sukhikh, G. T. (1998) *Tumor Biol. 19*, 30−40.
11. Semenkova, L. N., Dudich, E. I., and Dudich, I. V. (1997) *Tumor Biol. 18*, 261−273.
12. Semenkova, L. N., Dudich, E. I., Dudich, I. V., Shingarova, L. N., and Korobko, V. G. (1997) *Tumor Biol. 18*, 30−40.
13. Laderoute, M. P., and Pilarski, L. M. (1994) *Anticancer Res. 14*, 2429−2438.
14. Nunez, E. A. (1994) *Tumor Biol. 15*, 63−72.
15. Sonnenschein, C., Ucci, A. A., and Soto, A. M. (1980) *J. Natl. Cancer Inst. 64*, 1141−1146.
16. Soto, A. M., Murai, J. T., Siteri, P. K., and Sonnenschein, C. (1986) *Cancer Res. 46*, 2271−2275.
17. Mizejewski, G. J., Dias, J. A., Hauer, C. R., Henrikson, K. P., and Gierthy, J. (1996) *Mol. Cell. Endocrinol. 118*, 15−23.
18. Morinaga, T., Sakai, M., Wegmann, T. G., and Namaoki, T. (1983) *Proc. Natl. Acad. Sci. U.S.A. 80*, 4604−4608.
19. Luft, A. J., and Lorscheider, F. L. (1983) *Biochemistry 22*, 5971−5978.
20. Zizkovsky, V., Strop, P., Korcakova, J., Havranova, M., and Mikes, F. (1983) *Ann. N.Y. Acad. Sci. 417*, 49−56.
21. Gibbs, E. M., Zelinski, R., Boyd, C., and Dugaiczyk, A. (1987) *Biochemistry 26*, 1332−1343.
22. Nishio, H., and Dugaiczyk, A. (1996) *Proc. Natl. Acad. Sci. U.S.A. 93*, 7557−7561.
23. He, X.-M., and Carter, D. (1992) *Nature 358*, 209−215.
24. Feldhoff, R. C., and Peters, T. J. (1975) *Biochemistry 14*, 4508−4514.
25. Reed, G. R., Feldhoff, R. C., and Peters, T. J. (1976) *Biochemistry 15*, 5394−5398.
26. Feldhoff, R. C., and Ledden, D. J. (1983) *Biochem. Biophys. Res. Commun. 114*, 20−27.
27. Geisow, M. J., and Beaven, G. H. (1977) *Biochem. J. 161*, 619−625.
28. Bayard, B., Kerckaert, J. P., Fournier, C., Roux, D., and Biserte, G. (1979) in *Carcino-Embrionic Proteins* (Lehmann, F. G., Ed.) Vol. II, pp 291−296, Elsevier/North-Holland Biomedical Press, Amsterdam.
29. Uversky, V. N., Kirkitadze, M. D., Narizhneva, N. V., Potekhin, S. A., and Tomashevski, A. Yu. (1995) *FEBS Lett. 364*, 165−167.
30. Uversky, V. N., Narizhneva, N. V., Ivanova T. V., Kirkitadze, M. D., and Tomashevski, A. Yu. (1997) *FEBS Lett. 410*, 280−284.
31. Uversky, V. N., Narizhneva, N. V., Ivanova T. V., Kirkitadze, M. D., and Tomashevski, A. Yu. (1997) *Biochemistry 36*, 13638−13645.
32. Freire, E. (1995) *Methods Enzymol. 259*, 144−168.
33. Privalov, P. L., and Potekhin, S. A. (1986) *Methods Enzymol. 131*, 4−51.
34. Nishi, S. (1970) *Cancer Res. 30*, 2507−2513.
35. Nishi, S., and Hirai, H. (1972) *Biochim. Biophys. Acta 278*, 293−298.
36. Parmelee, D. C., Evenson, M. A., and Deutsch, H. F. (1978) *J. Biol. Chem. 253*, 2114−2119.
37. Ruoslahti, E., and Engvall, E. (1978) *Scand. J. Immunol. 7* (Suppl. 6), 1−17.
38. Bradford, M. M. (1976) *Anal. Biochem. 72*, 248−254.
39. Moos, M., Jr., Nguyen, N. Y., and Liu, T.-Y. (1988) *J. Biol. Chem. 263*, 6005−6008.
40. Provencher, S. W., and Glöckner J. (1981) *Biochemistry 20*, 33−37.
41. Dudich, I. V., Zav'yalov, V. P., Pfeil, W., Gaestel, M., Zav′ylova, G. A., Denesyuk, A. I., and Korpela, T. (1996) *Biochim. Biophys. Acta 1253*, 163−168.
42. Woody, R. W. (1995) *Methods Enzymol. 246*, 34−71.
43. Mizejewski, G. J. (1997) *Proc. Soc. Exp. Biol. Med. 215*, 333−362.
44. Mizejewski, G. J. (1995) *Crit. Rev. Eukariotic Gene Express. 5* (3, 4), 281−316.
45. Ptisyn, O. B. (1992) in *Protein Folding* (Creighton, T. E., Ed.) pp 243−300, W. H. Freeman & Co., New York.
46. Ptisyn, O. B. (1995) *Adv. Protein Chem. 47*, 83−229.
47. Dudich, I. V., Semenkova, L. N., Gorbatova, E. A., and Dudich, E. I. (1997) *Tumor Biol. 18* (S2), 101.
48. Dudich, I. V., Semenkova, L. N., and Dudich, E. I. (1997) *Tumor. Biol. 18* (S1), 86.
49. Dudich, E. I., Semenkova, L. N., Gorbatova, E. A. Dudich, I. V., Zubov, D. L., and Tatulov, E. B. (1998) *Tumor Biol. 19* (S2), 25.

BI990630H